Results in Engineering 10 (2021) 100214

Contents lists available at ScienceDirect

Results in Engineering

journal homepage: www.editorialmanager.com/rineng/Default.aspx

Experimental investigation of thermoelectric cooling for a new battery pack design in a copper holder

You Lyu, Abu Raihan Mohammad Siddique, S. Andrew Gadsden, Shohel Mahmud *

College of Engineering and Physical Sciences, University of Guelph, Canada

ARTICLE INFO

Keywords:
Electric vehicle
Li-ion battery
Battery thermal management system
Thermoelectric cooling
Liquid cooling
Forced air cooling

ABSTRACT

Solid-state thermoelectric refrigeration and heat pump systems can be integrated with battery packs in electric vehicles (EV) and hybrid electric vehicles (HEV) for effective thermal management in both hot and cold environments. Operating modes can be switched by changing the polarity of the input voltage to the thermoelectric system. In this paper, a new design of a battery pack is proposed which includes an acrylic battery container, copper battery holders, liquid cooling medium, and battery cells. This battery pack is integrated with a battery thermal management system (BTMS) which includes thermoelectric cooling (TEC) in combination with liquid and air circulations. The aim of the BTMS is to handle heat generation during operation of the battery pack. Heat, generated by the battery pack, is transported to the cold end of the TEC and then dissipated to the surrounding environment by a heatsink. Fundamental design optimization is carried out on a single cell first. System performance is then validated in the battery pack experiments. For the 40 V test, the proposed system reached approximately 20 °C lower when compared with only liquid cooling. In the 30 V power supply test, the battery pack temperature did not exceed 30 °C in a period of 5000 s. Furthermore, the battery pack temperature was under 60 °C at 3000 s during a continuous discharge condition with a 50 V input, which is considered an extreme condition for battery operation.

1. Introduction

The transportation sector which consists mainly of vehicles consumes approximately one-fifth of energy worldwide [1–3]. Among all of the available fuel choices worldwide, oil is the main source of energy generation. As of 2014, the International Energy Agency (IEA) reported that 93% of transportation used oil [4]. However, total fossil fuels reserves are limited on Earth. Petroleum, for instance, as an important primary energy resource and has been used for more than a century. Since oil yearly production is about 1% of total in-stock, it will not take another century to consume the remaining 78% world reserve amount [5]. At the same time, transport, which is responsible for about 23% of all energy-based carbon dioxide emissions, has caused significant environmental and social concerns [6]. Accordingly, researchers have been actively developing clean energy-based transportation systems to help overcome these issues.

Electric vehicles and hybrid electric vehicles (EV/HEV) utilize electricity-based generators and engines and have attracted enormous attention around the globe. Instead of petroleum, EV/HEV use a secondary energy source: electricity, which can be generated efficiently by multiple sources in a large scale. Renewable energy resources like wind and solar are becoming more wide spread, such that EV/HEV will reduce overall global emissions even further. A study predicted that from 2000 to 2030 an additional 530 million vehicles will be put on the road in India and China alone [7]. Hence, the need for EV/HEV to grow in popularity is important to offset the demand for vehicles. As of 2015, approximately 0.1% of the total number of vehicles were EV/HEV. However, it is anticipated that 40% of the total number of passenger vehicles will be EV/HEV by 2050 [8].

The main factors that limit the widespread adoption of EV/HEV is energy storage capacity, charge/discharge rates, and battery costs [9]. The performance of EV/HEV is largely dependant on the working status of the installed battery pack. For instance, the discharge capacity of the vehicle battery pack determines performance during vehicle acceleration. In addition, driving range relies heavily on the charging capacity of the battery cells. Among all of the types of rechargeable batteries, Li-ion batteries have high-energy density and excellence performance which make them attractive for HV/HEV applications [10]. Currently, one of the highest Li-ion battery energy densities is about 300 Wh/kg, which has tripled over the past three decades [11]. However, some safety

* Corresponding author.
E-mail address: smahmud@uoguelph.ca (S. Mahmud).

https://doi.org/10.1016/j.rineng.2021.100214
Received 29 January 2021; Accepted 2 March 2021

concerns are present in Li-ion batteries such as overheating which causes fires and, on rare occasions, explosions [12]. Cell battery and pack temperature is an important feature which is critical to battery operation as the energy density and charge/discharge rate increases. Both the battery charge/discharge process and its lifespan are dramatically dependent on temperature. According to Ref. [13], Li-ion batteries should be operated within a temperature range of 15-35 °C. An operating temperature of over 50 °C should be avoided at all time because high temperatures have negative effects on the battery itself which reduces its remaining useful life [14]. Furthermore, failing to manage battery thermal behaviour properly may lead to dangerous thermal runaway scenarios causing battery failures.

Batteries generate a certain amount of heat which increases the operating temperature. There are two main sources that increase battery internal heat generation: 1) entropy changes caused by electrochemical reactions, and 2) resistance-based Ohmic heating [15]. While the current flows, the volume difference between battery heat generation and dissipation determines the change of battery temperature [16]. Two scenarios that need to be minimized to improve battery efficiency include: 1) rapid temperature rises during charging and discharging, and 2) uneven temperature distributions across battery cells and pack.

Battery thermal management systems (BTMS) are designed to maintain battery temperatures within a healthy operating range [17]. Recognized BTMS practices can be divided into two groups, namely, passive and active methods [18]. Passive methods do not use energy to dissipate heat, they typically employ phase change materials (PCMs) [19], heat pipes [20], and hydrogels [21] to remove excess heat from the battery. Active methods, on the other hand, consume a certain amount of energy while operating a fan for air flow [22] or pump for coolant circulation [23]. Regardless of energy consumption, active methods are considered more flexible and are highly controllable.

Thermoelectric coolers (TECs) transfer heat from the cold-end to the hot-end of the material whenever electricity is applied. TECs are well-known for its reliability and manageability and can be easily controlled to manage the temperature of specific battery cells. For EV and HEV applications, this feature is considered highly favourable as the temperature may fluctuate significantly in specific locations. Although applications are already found in consumer electronics and fossil-energy powered automobiles [24], research in managing battery temperatures are still needed. In 2003, researchers purposed a design for battery cooling that made use of blowing air from the TEC cold-end into the battery chamber [25]. It is desirable to attach the TEC cold-side directly onto the battery surface to make the cooling action more efficient [26], or to the battery tabs to decelerate battery degradation activities [27]. A design that utilized direct contact with the battery at the cold-end and water cooling at the hot-end was able to maintain cell temperature 5-8 °C lower compared to the water cooling method where the environmental temperature was 40 °C [28]. Regarding parameter optimization, a study showed that the arrangement of a heatsink fan on the TEC hot-end largely impacts the overall cooling efficiency [29]. Another article suggests power consumption could be reduced by implementing a temperature control strategy [30]. A recent study introduced a design that used liquid coolant as the heat transfer medium between the battery and the TEC module which has forced air assistance from its condenser side. Experimental results on a single simulated cell with copper holder protection offered a 43 °C temperature drop on the cell surface [31].

As the popularity of EV/HEVs grow, improved ride quality and operating performance are becoming more important. To improve performance, higher charge/discharge speeds are required, as well as greater energy storage capacity. The heat dissipation rate of single cells and the quantity of on-board batteries are increased significantly for better vehicle performance. Some research has shown that forced air cooling has difficulty reaching the cooling goal for mass battery packs being discharged at high speeds [32]. Advanced BTMS designs are in high demand within both academia and industry. A new BTMS design of TEC liquid forced air was introduced in Ref. [32], and proved the enhanced cooling performance compared to liquid cooling for heat dissipation by a single cell [31].

The purpose of this paper is to investigate the key design parameter for a proposed BTMS based on a single cell. A new battery pack design is presented which is suitable for generating an enormous amount of heat in a short period of time. Experimental assessments are then carried out to study the thermal management capability for battery packs in both charging/discharging and idle status. A numerical uncertainty analysis is performed to evaluate the accuracy of the output data from each test. The paper is organized as follows. Section 2 provides a summary of the fundamentals of thermoelectric cooling. The experimental setup is described in detail in Section 3. The results of running the experiment are shown in Section 4, and Section 5 provides the numerical uncertainty analysis. In Section 6, the paper is then concluded.

2. Fundamentals of thermoelectric cooling

The Peltier effect is the main working principle for thermoelectric cooler/heat pumps and converts electrical energy into a temperature gradient. A certain amount of temperature differences are expected between the cold and hot-ends of a thermoelectric module whenever an electric current is applied. Fig. 1 shows a simplified structural of a typical thermoelectric cooler; it only involves two pairs of legs. As shown in the left-half of the figure, the basic unit of a TEC consists of a semiconductor p-type leg, a semiconductor n-type leg, and a metal connector. The spare end of the p-type leg is connected to the n-type leg of the next unit and the unused side of the n-type is connected to another p-type spare-end of the neighbouring unit. Two thermally conductive plates that function as electric insulators are added to convert it into a sandwich structure [33].

All of these portable components are noise and maintenance-free which make TEC a reliable and efficient candidate for cooling. When an electric current flows in the direction shown in Fig. 1, the thermoelectric module absorbs heat from the cold-end at the top, and releases heat to the hot-end at the bottom. The Peltier heat can be expressed asQp = ∏I $Q_p = \Pi I$ (1), where Q_p, Π, and I refer to the Peltier heat, the Peltier coefficient, and electric current, respectively. Therefore, the TEC thermal behaviour can be controlled by altering the supplied current. Moreover, if the carriers move in the opposite direction to the case shown in Fig. 1, the previous hot-end will be working as the cold-end, and will start absorbing heat immediately. This makes it possible to turn a TEC cooler into a heater without any delay, such as in EV/HEV applications.

The commercial TEC model (TEC1-12708) adopted in this study has a total of 127 couples that are connected electrically in series and thermally in parallel. It has a rated maximum heat pump capacity of 85 W. Two ceramic plates are installed in place to cover the top and the bottom of these connected couples. A pair of electrical wires, prepared by the manufacturer, supply DC power from the outside environment.

3. Experimental setup

The battery pack system is designed and constructed ideally for

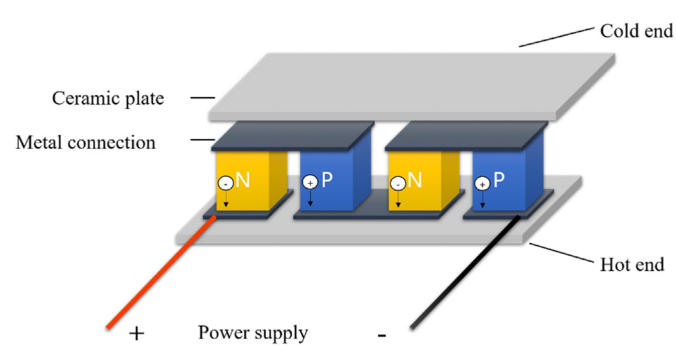

Fig. 1. Schematic of the thermoelectric module.

laboratory scale experiments in order to assess the performance of advanced cooling systems. The experimental setup is especially suitable for the simulation of the cell pack charge/discharge process where a substantial amount of heat is internally created in a very short period of time. The TEC liquid forced air assisted BTMS is divided into two sections, namely, a TEC subsystem and a liquid flow subsystem. The TEC subsystem consists of two thermoelectric coolers, an aluminum heatsinks, and two axial cooling fans. The liquid flow subsystem contains a general-purpose waterproof pump to circulate the liquid coolant and a set of plastic pipes to form the liquid flow path. An overview of the experimental setup with the battery pack arranged in the BTMS is shown in Fig. 2. For every experiment, all of the devices and instruments are arranged in a laboratory in which the room temperature fluctuates mildly between 20 and 25 °C. The laboratory uses standard air pressurization.

3.1. TEC sub-system

In terms of thermal behaviour management, the TEC subsystem is a crucial part of the TEC liquid forced air system. The TEC subsystem is responsible for removing the heat transported by the cooling liquid to the environment outside of the BTMS. As shown in Fig. 3, there are two identical TECs employed in the system to move heat physically from the same side to the other. An aluminum block, which is attached to the heat-absorbing-end of each TEC, and contains a U-shaped fluid channel. The outlet of one channel is connected to the inlet of the adjacent fluid channel to arrange the connection in series. These channels host the heat exchange between the TEC module and the cooling liquid. All of the TECs and aluminum blocks are secured onto the heatsink by bolts, nuts, and aluminum strips. Plastic sleeves are properly prepared to avoid direct contact, and thus heat exchange is prevented between the cold and hot side. For the hot-end of the TECs, an aluminum fin heatsink structure is firmly attached. Two DC brushless fans are fastened closely to the end of heatsink fins. The heatsink takes the rapidly accumulating heat away from the TECs quickly when the system is in operation. The two fans, at the far-end, are used to assist the heatsink to suppress the temperature of the TECs. However, this heat removal strategy of the TEC hot-end may be insufficient if the power dissipation amount is extremely high; a more aggressive method is needed to resolve this bottleneck.

3.2. Liquid flow sub-system

Coolant is used as the heat exchange medium between the batteries/battery pack and the TEC subsystem. Due to safety and cost concerns, water was deployed in this study as the coolant. The designated coolant flow path is found in Fig. 4. All of the components are connected in series by uniform transparent plastic pipes for coolant circulation. Note that the fluid channels of the two aluminum blocks are also connected in serial via a plastic pipe. To move the coolant flow, a brushless DC pump with a rated horizontal capacity of 4 L per minute is added into the liquid flow path. A calibration for pump capacity of driving water flow was carried out in the laboratory before attaching the pump to the cooling system. Even though the container and the pipes are deliberately chosen to be transparent for convenient monitoring, it may still be desirable to equip a flowmeter in an advanced BTMS to obtain real-time water flow rate measurements in real applications. This information could be fed-back into the BTMS for optimizing flow rates and condition monitoring.

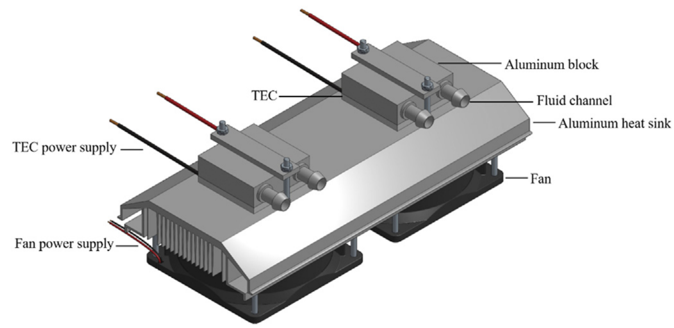

Fig. 3. Structure of the TEC sub-system.

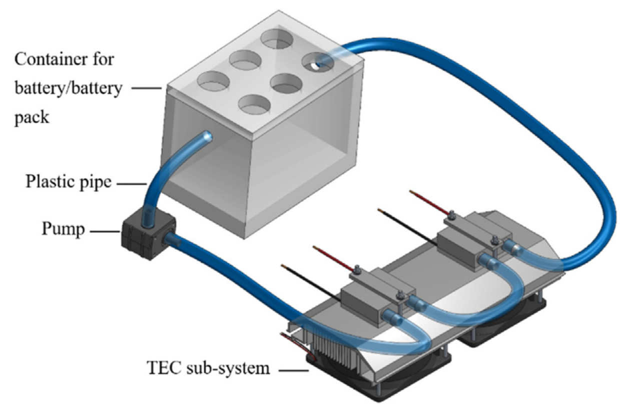

Fig. 4. Illustration of the coolant flow path.

3.3. Battery pack simulation set

The single battery/simulated battery are both commonly used by researchers to assess the performance of a BTMS. On the other hand,

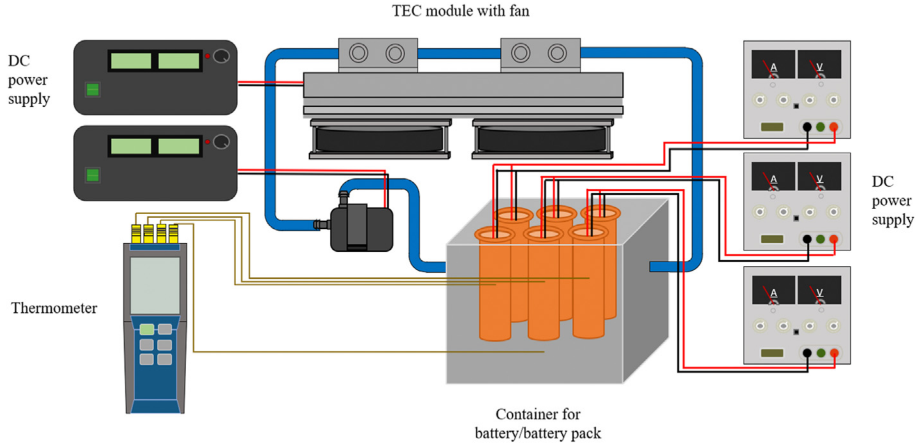

Fig. 2. Schematic presentation of an overview of the experiment setup.

commercially available EV/HEV like the Nissan Leaf and Chevrolet Volt are generally loaded with battery packs made by hundreds of Li-ion batteries [34]. An enormous amount of heat generation can be expected during a short period of normal operation. Consequently, a single cell is vastly inadequate to fully evaluate the ability of a well-developed BTMS. Furthermore, it is useful to investigate the thermal inter-relation among single cells and the temperature uniformity across the whole pack. Therefore, it is desirable to develop a battery/simulated battery pack with reasonable heat generation rates to test the thermal behaviour of a modern BTMS.

The newly developed battery pack simulation setup utilized simulated cells. With real batteries, all of the experiments must be carefully designed and operated to avoid any extreme conditions that may lead to severe thermal runaway. This limits the quantity and quality of permitted tests. By contrast, simulators can handle extreme conditions while the thermal behaviour remains similar to real batteries. A total of six cells were manufactured from an aluminum rod to match the size of the well-known cylindrical 21700 Lithium-ion battery commonly used in the EV/HEV industry. At the center of the top face for each cell, a cylindrical hole was drilled to fit in the selected heater. A study monitored a 6Ah cylindrical cell discharged at 10 °C and found that the heat generation rate was 41.6 W [35]. Another study reported that the heat generation rate of a charging Li-ion battery at 8 °C reached 54.4 W [36]. The heater chosen for the simulated battery has a rated power of 100 W (CSH-102100, OMEGA Engineering). Thermal paste was used to cover the surface of each heaters before being into the pre-drilled chamber of the simulated cell.

As shown in Fig. 5, copper holders were constructed to prevent the battery pack from directly contacting the surrounding coolant. By introducing the holders, corrosion and safety concerns from circulating coolant on the real batteries can be minimized. The high-thermal conductivity of copper may help to reduce the imbalanced distribution of battery surface temperatures while in operation. All of the copper holders were carefully prepared to hold the cells tightly inside; any gap between the copper holder and the aluminum simulator was evenly filled by thermal paste.

An acrylic container was prepared for the battery/battery pack and was used to store the extra cooling liquid. The heat generated by operating the battery/battery pack was passed to the coolant in this container. The circulating pump moved the heated coolant to the TEC subsystem where the heat was dissipated into the environment. Chilled coolant was moved to refill the container and reduce the temperature of the heated battery/battery pack. As shown in Fig. 5, a removable lid was drilled with six battery-sized holes for all of the battery pack experiments. There were three rows of batteries in the container (along the liquid flow-direction), and the distance from the inlet to the two cells in the same row was identical. Glue was utilized to hold the battery pack at a certain height to allow for the coolant to flow through the space underneath. Two holes were drilled on the side walls of the container for the inlet and outlet paths for the cooling liquid; as the coolant flow directions were fixed for each test.

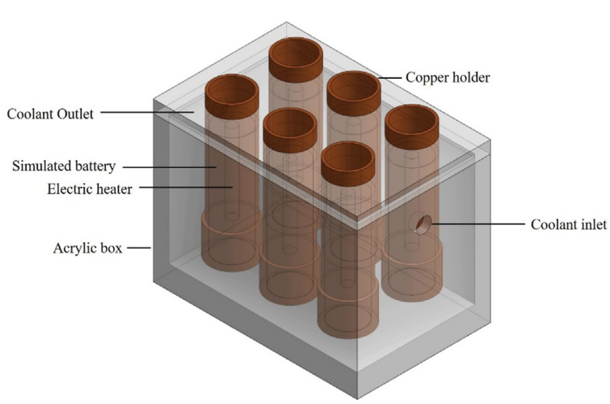

Fig. 5. Structure of the battery pack simulation set.

4. Experimental tests and results

Detailed experimental studies were implemented in two sectors: 1) single cell, and 2) battery pack. The single battery experiments were developed to optimize the operating parameters of the purposed BTMS. A simulated battery pack was designed and implemented in the laboratory to study the thermal management capabilities of modern BTMS'. Based on the battery pack, various battery working conditions were considered and tested in the TEC-based BTMS.

4.1. Simulated single battery

The experiments included in this section were based on a single simulated cell. Table 1 summarizes the operational variables for the TEC-based BTMS. Among these parameters, the heater power supply value was only changed in tests to incorporate the battery pack. The influence of changing TEC power supply values (8 V, 10 V, and 12 V) to system cooling performance was evaluated in a previous experiment, and a certain degree of difference in cooling effect was expected if the TEC voltage supply was changed [31]. The following experiments focus on investigating the impact to the BTMS with varied power supplies to the cooling fan as well as the circulating pump.

4.1.1. Single cell in copper casing (with different fan supply voltages)

Control parameters and variables like air flow rate and internal heat generation of the cooling fan can be controlled by varing the supplied power. The influence of changing the power supply values to the cooling fan, the TEC sub-system, and the BTMS is examined in this section. The voltage supplied to the pump and the TEC module was fixed to 10 V while, to the cooling fan, it was started from 8 V in the first test, and increased to 10 V and 12 V in subsequent tests. Detailed power supply settings of each module in the TEC-based BTMS is found in Table 2.

An OMEGA four-channel data logging thermometer (HH374) with K-type thermocouples was utilized in this study for measuring and recording the temperatures. Thermocouples were placed to monitor the temperature of the inner- and outer-sides of the copper casing, coolant in the container, and the surrounding air. As shown in Fig. 6, the temperature readings from inside the copper holder, outside the copper holder, and water of all three tests declined remarkably after 90 min in operation. The temperature difference between the thermocouples inside and outside the copper holder was generally lower than 0.5 °C. Among the three tests with different supplied fan voltages, the lowest battery surface temperature ever reached (10.4 °C) was in the 8 V test. However, it was noticeable that the initial temperature inside the holder for the 8 V fan test (19.4 °C) was also slightly lower than the 10 V (22.2 °C) and 12 V (19.8 °C) tests.

Table 1
Variables of simulated battery experiments.

Equipment	Variables
Battery	Power supply of heater
Thermoelectric cooler	Power supply
Cooling fan	Power supply
Liquid pump	Power supply

Table 2
Parameters of single cell in copper casing test (with varying fan supply voltages).

Variable	Heater	TEC	Pump	Fan
Voltage/Current	40 V/0.05A	10 V/6.7A	10 V/0.3A	8 V/0.41A 10 V/0.5A 12 V/0.54A

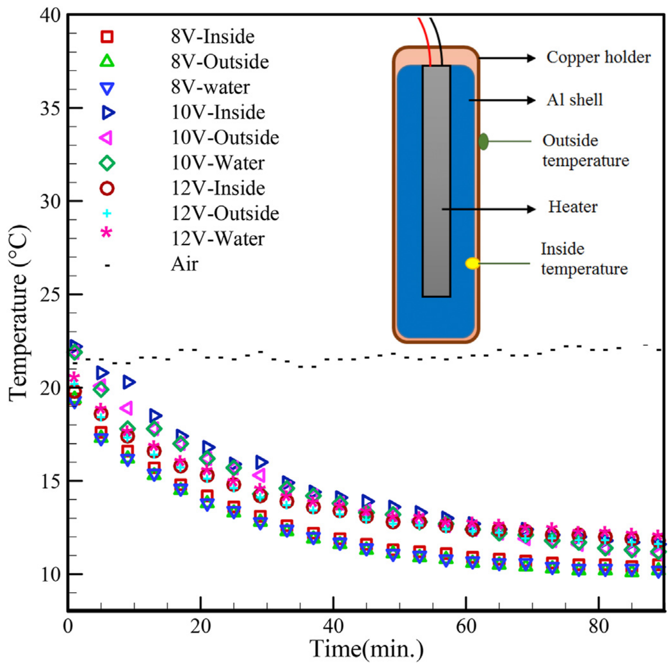

Fig. 6. Temperature versus time for a single battery in copper casing in TEC-based cooling experiments (varying fan voltages from 8 V, 10 V–12 V, 40 V constant battery power supply).

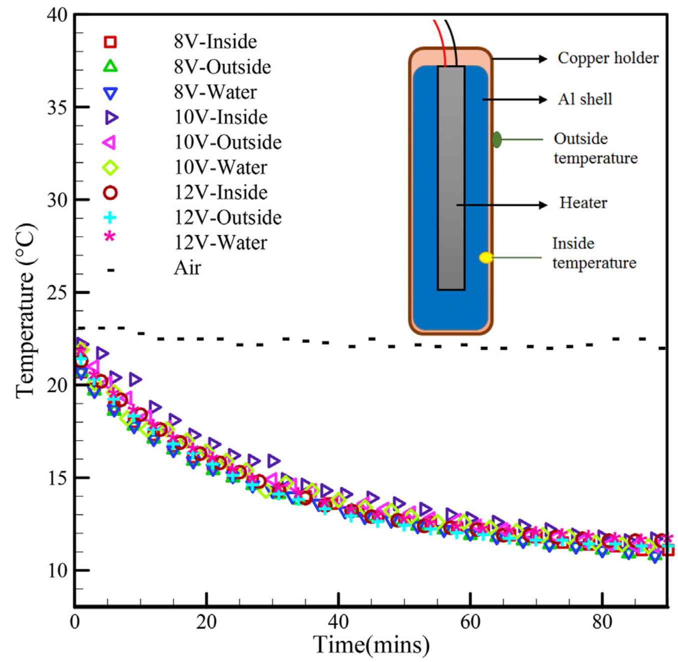

Fig. 7. Temperature versus time for single battery in copper casing test (varying pump voltage from 8 V, 10 V–12 V, 40 V constant power supply for battery).

The overall temperature drop was calculated by subtracting the final temperature at 90 min from the initial temperature of the same position in each test. The largest drop of overall temperature (inside the holder) was reached with the 10 V test (10.6 °C), followed by the 8 V (8.9 °C), and the 12 V (8 °C) tests. For the first 30 min of the tests, the cooling effect of the 8 V fan (cell temperature lowered 6.3 °C) was nearly as strong as the 10 V fan (cell temperature lowered 6.2 °C). As contrast, the 12 V fan only lowered the cell temperature 5.6 °C during the same period. If we only examine the final 30 min of each test, the cooling effect of the 10 V fan (cell temperature lowered 4.3 °C) surpassed its competitors. In the same period, the 8 V and 12 V fans only cooled the battery 2.4 °C lower compare with the starting points.

4.1.2. Single cell in copper casing (with different pump supply voltages)

The power supplied to the liquid pump also impacted the performance of the TEC-based BTMS. Theoretically, the change of power supply to a pump can impact both the fluid flow speed and the pump internal-heat generation rate. The following experiments were designed to evaluate the impact to the cooling system by changing the power supplied to the circulating pump. In these tests, the power supplied to the fan and TEC module were fixed at 10 V.

The system response with varied power supply to the pump is shown in Fig. 7. Four thermocouples were used to monitor the temperature of the battery surface, the copper holder, water, and ambient air. As shown in Fig. 7, the cooling effect change of varying the pump voltage was milder than varying the fan voltage. Based on the overall temperature decline (from test start to finish), the 10 V pump yielded the best ability for cooling. With the 10 V powered pump, the battery surface temperature dropped to 10.6 °C in 90 min, while the copper holder surface temperature dropped to 10.8 °C in the same period. For the 8 V powered pump test, the temperature dropped to 9.6 °C at the battery surface and 9.9 °C at the copper holder surface, for a period of 90 min. For the pump provided with 12 V, after 90 min, it lowered the temperature of the battery surface to 9.7 °C and the holder surface to 10.1 °C. The variation of voltages and currents of different components is listed in Table 3.

Table 3
Parameters of cell in copper casing test (varying pump supply voltages).

Variable	Heater	TEC	Fan	Pump
Voltage/Current	40 V/0.05A	10 V/6.7A	10 V/0.48A 10 V/0.5A 10 V/0.49A	8 V/0.24A 10 V/0.3A 12 V/0.37A

4.2. Simulated battery pack

A battery pack with six simulated batteries was designed and prepared for comprehensively testing an advanced BTMS. It was designed to investigate the ability of a BTMS to manage the vast amount of heat dissipation from batteries as well as the temperature distributions across a battery pack. In this section, experiments were completed with this simulated battery pack for the proposed TEC-based BTMS.

4.2.1. Battery pack in liquid cooling/TEC-based cooling

The tests recorded and presented in this section were intended to compare the cooling effect of the pure liquid with the TEC liquid forced air. With constant power supplied (40 V) to the heater, temperature measurements were collected and plotted in Fig. 8. As illustrated in Fig. 8, the batteries in the pack were divided into three rows per spatial distribution. One thermocouple was vertically attached to the middle of a battery (surface of the copper casing) in each row. There was an additional thermocouple arranged in the container for monitoring the coolant temperature. The data logging frequency for the thermometer was set to 1 Hz. Each of the two experiments (with and without the TEC module) lasted 5000 s and the results are plotted in Fig. 8.

In the pure liquid cooling test, the highest temperature feedback obtained was 60.7 °C, and was from the thermocouple attached to the cell horizontally in the center of the container (Row 2). The temperature of the cell next to the outlet (Row 3) reached 60 °C, and the water temperature reached 58.8 °C in the same amount of time. The cell beside the inlet (Row 1) experienced the lowest temperature and was recorded as 58.2 °C at 5000 s. However, the water temperature remained the lowest for most of the test period, and it surpassed the temperature measured from Row 1 during the last 1000 s. Based on the results, it

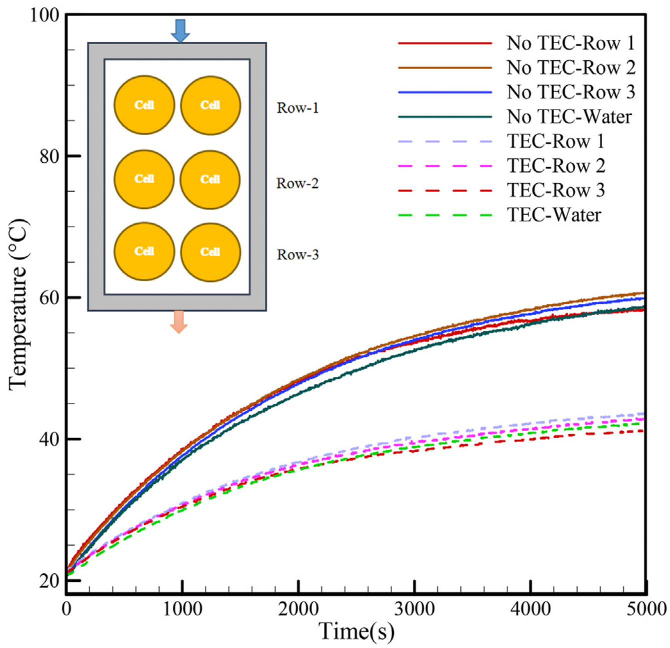

Fig. 8. Temperature versus time for the battery pack in the copper casing in liquid cooling and TEC based cooling tests (40 V constant power supply for the heater).

appears the cooling effect of pure liquid was not satisfied for the proposed battery pack since such a high temperature could damage the cell. Another test utilized the TEC subsystem which improved the overall cooling effects. Temperature readings at 5000 s for Row 1, Row 2, Row 3, and the water was recorded at 43.7 °C, 42.8 °C, 41.2 °C, and 42.3 °C, respectively. For the first 2500 s, the water temperature was marginally-lower than the Row 3 temperature. Nevertheless, it exceeded the Row 3 battery temperature for the remaining 2500 s. The greatest temperature difference recorded between any two cells in the pack was 2.6 °C during this 5000 s interval. Table 4 shows the voltage and current consumption of heater, TEC, and fan and pump.

4.2.2. Battery pack in TEC-based cooling (with different heater supply voltages)

The cooling capacity of the TEC-based BTMS was tested in this section by varying the power supply to the heater of the cells in the simulated battery pack. In a stable environment, a modest increase of the voltage supplied to the electric heater will increase its heat generation and surface temperature. In this section, to explore the temperature management limits of the TEC-based cooling system, the power supplied to the heater was increased from 30 V, to 40 V, and finally to 50 V. The experimental results are shown in Fig. 9. The power supplied to the fan, the liquid pump, and the TEC was maintained at 10 V. The battery temperature was suppressed to under 30 °C in the 30 V heater power supply test. When the heater voltage was increased to 40 V, the maximum cell surface temperature reached was 43.7 °C. With a constant supply voltage of 50 V, the temperature was predicted to rise quickly. The data collected showed that the highest temperature reached 62.2 °C at Row 1; this temperature was considered to be harmful to the cell. The maximum cell temperature difference (3 °C) was reached by Row 1 and Row 3. The largest temperature difference between the water and any cell during this test was 5.4 °C, recorded at 4989 s. For the first 2000 s, the temperature of any monitored battery in the pack was maintained under 50 °C. Based on these test results, the proposed TEC-based cooling system was able to keep the batteries healthy during a continuous charge/discharge cycle. The power consumption of each component is presented in Table 5.

Table 4
Parameters of battery pack test.

Variable	Heater	TEC	Fan & Pump
No TEC-Voltage/Current	40 V/0.59A	–	10 V/0.8A
TEC-Voltage/Current		10 V/6.6A	

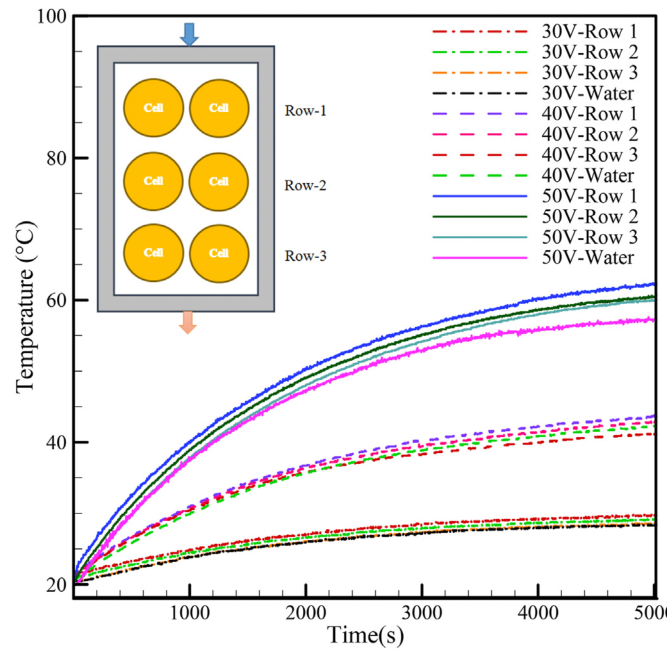

Fig. 9. Temperature versus time for the battery pack in the copper casing in TEC based cooling test (varying heater voltage supply from 30 V, 40 V–50 V).

Table 5
Parameters of battery pack test (varying heater voltage).

Variable	Heater	TEC	Fan & Pump
Voltage/Current	30 V/0.44A	10 V/6.3A	10 V/0.8A
	40 V/0.59A	10 V/6.6A	
	50 V/0.74A	10 V/6.4A	

4.2.3. Abusive charge/discharge scenarios

The final scenario abusively charged/discharged the battery pack for more than 6000 s. During the charge/discharge process, the power supply to the heater was kept constant at 50 V. The power supply to the TEC, pump, and fan was held constant at 10 V. The results of these tests are shown in Fig. 10. Once the heaters were activated, the measured temperatures from all of the thermocouples rose rapidly. After 2000 s, the rise of battery pack temperature began to slow. The highest battery temperature logged during the test was 63.6 °C in Row 1. Once the power supplied to the heaters were removed, at around 6350 s, the temperatures began to rapidly drop. Approximately 840 s later, the TEC-based BTMS cooled down the battery pack to 50 °C. After an additional 525 s, the battery pack temperature decreased further from 50 °C to 40 °C.

In real applications, the battery thermal behaviour in the first part of the test corresponds to an abusive usage of the battery pack or an emergency caused by thermal failure. The second part reveals the ability of the BTMS to cool-down the battery from an exceptionally high temperature. In these scenarios, it is desirable to quickly decrease the battery pack temperature to avoid critical or permanent damage to the cells. The removal of the heater power supply matches the state of a vehicle in deceleration. The battery pack installed on a vehicle needs to be well-prepared for the next period of acceleration; a reliable BTMS needs to remove the accumulated battery pack heat. The voltage and current

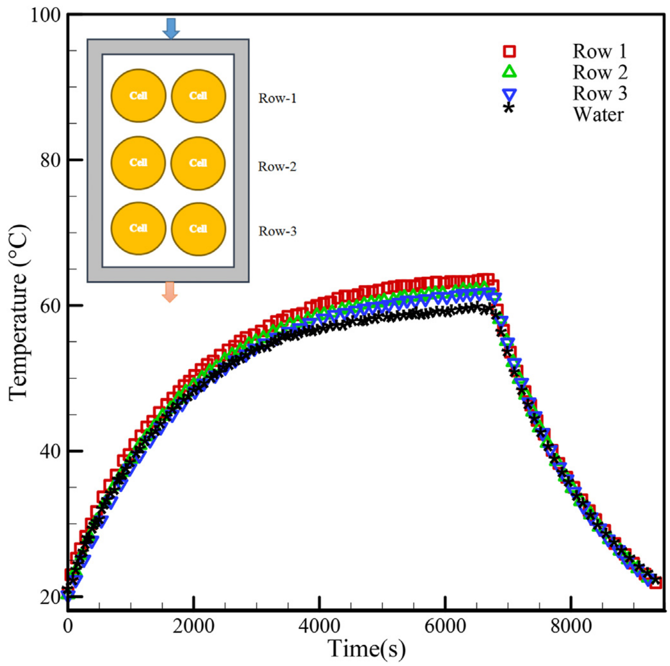

Fig. 10. Temperature versus time for the battery pack in copper casing worst-case scenario test (50 V power supply for the heater).

required by the components are listed in Table 6.

5. A brief uncertainty analysis

This study utilized (1) as the principal method to numerically analyze the impact of equipment accuracy on the experimental results [37]. Table 7 summarizes the uncertainty analysis of the experimental results. As an example, a peak battery temperature of 43.7 °C was reached in the battery pack in the TEC-based cooling test (40 V for heater, 10 V for TEC, fan, and pump). The calculated overall device uncertainty was approximately 0.055%.

$$s = \left\{ (s_1/m_1)^2 + (s_2/m_2)^2 + \cdots + (s_n/m_n)^2 \right\}^{0.5} \quad (1)$$

where, s represents the relative uncertainty, s_1, s_2, …., s_n represents accuracy of the sensors used in the experiment, and m_1, m_2, …., m_n represents the measured value by the sensors.

6. Conclusions

In this paper, a new battery pack with simulated batteries was designed and implemented in order to test modern battery thermal management systems. The pack contained six cells that were made of aluminum rods and electric heaters. Each cell was covered by a copper holder which protected it from the circulating coolant. A plastic container was specifically prepared for heat exchange between the battery pack and the selected coolant. An advanced hybrid cooling system which contains TEC, liquid cooling, and forced-air cooling was tested with the newly proposed battery pack. In this TEC-based cooling system, the forced-air cooling TEC module was responsible to deliver heat to the ambient environment.

The earliest experiments focused on design parameter optimization of the TEC-based BTMS. The results showed that the value of the voltage supplied to the fan and pump has noticeable impacts on the cooling system performance. Comparatively, varied power supplies of the cooling fan revealed a more significant change in battery temperature compared to the pump. BTMS performance validations were also carried out with the simulated battery pack. With 40 V power supplied to the heathers, the TEC-based BTMS was able to keep the battery pack roughly 20 °C lower than pure liquid cooling. The final experiment involved an extreme battery pack scenario. This experimental study revealed the ability of the BTMS to cool-down the battery from an exceptionally high temperature.

Future work includes an in-depth BTMS examination with typical charge/discharge cycles for EV/HEV systems, and the study of a cooling system control strategy for real-time parameter optimization. Furthermore, a thermal model will be established for convenient numerical simulations.

Table 6
Parameters of battery pack cooling down test.

Variable	Heater	TEC	Fan & Pump
Voltage/Current	50 V/0.73A	10 V/6.3A	10 V/0.8A

Table 7
Uncertainty analysis of experimental results.

Sensors	Accuracy ± (%)	Measured Value	Relative Uncertainty ± (%)
Thermometer	1 [°C]	43.7 °C	0.0229
Power Supply (Heater)	0.01 [V]	10 V	0.001
Power Supply (Others)	2 [V]	40 V	0.05

Credit role

You Lyu: Conceptualization, Methodology, Investigation, Writing – Original Draft. **Abu Raihan Mohammad Siddique**: Methodology, Instruction, Formal Analysis, Consultation, Review and Editing. **S. Andrew Gadsden**: Co-Supervision, Project Management, Review and Editing. **Shohel Mahmud**: Supervision, Project Management, Funding Acquisition, Writing- Review and Editing.

Declaration of competing interest

The authors declare that they have no known competing financial interests or personal relationships that could have appeared to influence the work reported in this paper.

References

[1] S. Bilgen, Structure and environmental impact of global energy consumption, Renew. Sustain. Energy Rev. (2014).
[2] A. Karnama, ENergy X.0: future of energy system, Results Eng. 3 (2019).
[3] A. Garcia, J. Monsalve-Serrano, Analysis of a series hybrid vehicle concept that combines low temperature combustion and biofuels as power source, Results Eng. 1 (2019).
[4] R.G. Newell, Global Energy Outlook, National Bureau of Economic Research, Cambridge, Mass, 2015.
[5] J. Riva, World Petroleum Resources and Reserves, Routledge, 2019.
[6] author., International Energy Agency, Energy Technology Perspectives 2017 : Catalysing Energy Technology Transformations, IEA, Paris, 2017.
[7] G. Fontaras, Z. Samaras, On the way to 130 g CO2/km-Estimating the future characteristics of the average European passenger car, Energy Pol. 38 (4) (2010) 1826–1833.
[8] Global EV Outlook 2016, 2016.
[9] G. Berckmans, M. Messagie, J. Smekens, N. Omar, L. Vanhaverbeke, J. Van Mierlo, Cost Projection of State of the Art Lithium-Ion Batteries for Electric Vehicles up to 2030, Energies, 2017.
[10] M. Yoshio, R.J. Brodd, A. Kozawa, Lithium-ion Batteries, vol. 1, Springer, 2009.
[11] H. Li, Practical evaluation of Li-ion batteries, Joule 3 (4) (2019) 911–914.
[12] Q. Wang, P. Ping, X. Zhao, G. Chu, J. Sun, C. Chen, Thermal runaway caused fire and explosion of lithium ion battery, J. Power Sources (2012).
[13] S. Ma, et al., Temperature effect and thermal impact in lithium-ion batteries: a review, Prog. Nat. Sci.: Mater. Int. (2018).
[14] T.M. Bandhauer, S. Garimella, T.F. Fuller, A critical review of thermal issues in lithium-ion batteries, J. Electrochem. Soc. (2011).
[15] I. Dincer, H.S. Hamut, N. Javani, Thermal Management of Electric Vehicle Battery Systems, John Wiley & Sons, 2016.

[16] H.A. Kiehne, Battery Technology Handbook, vol. 118, CRC Press, 2003.
[17] A.A. Pesaran, Battery thermal management in EV and HEVs: issues and solutions, Batter. Man 43 (5) (2001) 34–49.
[18] Z. Rao, S. Wang, A review of power battery thermal energy management, Renew. Sustain. Energy Rev. 15 (9) (2011) 4554–4571.
[19] R. Liu, J. Chen, J. Xun, K. Jiao, Q. Du, Numerical investigation of thermal behaviors in lithium-ion battery stack discharge, Appl. Energy 132 (2014) 288–297.
[20] A. Greco, D. Cao, X. Jiang, H. Yang, A theoretical and computational study of lithium-ion battery thermal management for electric vehicles using heat pipes, J. Power Sources 257 (2014) 344–355.
[21] R. Zhao, S. Zhang, J. Gu, J. Liu, S. Carkner, E. Lanoue, An experimental study of lithium ion battery thermal management using flexible hydrogel films, J. Power Sources 255 (2014) 29–36.
[22] T. Wang, K.J. Tseng, J. Zhao, Development of efficient air-cooling strategies for lithium-ion battery module based on empirical heat source model, Appl. Therm. Eng. 90 (2015) 521–529.
[23] M.R. Giuliano, S.G. Advani, A.K. Prasad, "Thermal analysis and management of lithium–titanate batteries, J. Power Sources 196 (15) (2011) 6517–6524.
[24] D. Zhao, G. Tan, A review of thermoelectric cooling: materials, modeling and applications, Appl. Therm. Eng. 66 (1–2) (2014) 15–24.
[25] Z.M. Salameh, C. Alaoui, "Modeling and simulation of a thermal management system for electric vehicles," in Industrial Electronics Society, in: IECON'03. The 29th Annual Conference of the IEEE, 2003, vol. 1, 2003, pp. 887–890.
[26] C. Alaoui, Solid-state thermal management for lithium-ion EV batteries, IEEE Trans. Veh. Technol. 62 (1) (2013) 98–107.
[27] I.A. Hunt, Y. Zhao, Y. Patel, G.J. Offer, Surface cooling causes accelerated degradation compared to tab cooling for lithium-ion pouch cells, J. Electrochem. Soc. 163 (9) (2016) A1846–A1852.
[28] Y. Liu, S. Yang, B. Guo, C. Deng, Numerical analysis and design of thermal management system for lithium ion battery pack using thermoelectric coolers, Adv. Mech. Eng. 6 (2014) 852712.
[29] S.Y. Kim, K. Lee, S. Park, J. Kim, "Thermal Design Analysis and Performance Test of a 1kW Thermoelectric Battery Cooler," in Thermal and Thermomechanical Phenomena in Electronic Systems (ITherm), IEEE Intersociety Conference on, 2014, pp. 1417–1421.
[30] C.-W. Zhang, K.-J. Xu, L.-Y. Li, M.-Z. Yang, H.-B. Gao, S.-R. Chen, Study on a battery thermal management system based on a thermoelectric effect, Energies 11 (2) (2018) 279.
[31] Y. Lyu, A.R.M. Siddique, S.H. Majid, M. Biglarbegian, S.A. Gadsden, S. Mahmud, Electric vehicle battery thermal management system with thermoelectric cooling: a case study, Case Stud. Therm. Eng. (2018).
[32] G. Xia, L. Cao, G. Bi, A review on battery thermal management in electric vehicle application, J. Power Sources 367 (2017) 90–105.
[33] C.M. Bhandari, D.M. Rowe, CRC Handbook of Thermoelectrics, vol. 49, CRC Press, Boca Raton, FL, 1995.
[34] C. Yuan, Y. Deng, T. Li, F. Yang, Manufacturing energy analysis of lithium ion battery pack for electric vehicles, CIRP Ann. - Manuf. Technol. (2017).
[35] A.A. Pesaran, M. Keyser, Thermal characteristics of selected EV and HEV batteries, in: Proceedings of the Annual Battery Conference on Applications and Advances, 2001.
[36] Y. Ye, L.H. Saw, Y. Shi, A.A.O. Tay, Numerical analyses on optimizing a heat pipe thermal management system for lithium-ion batteries during fast charging, Appl. Therm. Eng. 86 (2015) 281–291.
[37] R.J. Moffat, Describing the uncertainties in experimental results, Exp. Therm. Fluid Sci. 1 (1) (1988) 3–17.